

Reactions $\gamma\gamma \rightarrow \pi\pi$ and $\gamma\gamma \rightarrow K\bar{K}$: the $(IJ^{PC} = 00^{++})$ -wave spectra at $E_{\gamma\gamma}^{(c.m.)} \sim 300 - 1900$ MeV

A.V.Anisovich and V.V.Anisovich

St.Petersburg Nuclear Physics Institute, Gatchina, 188350, Russia

Abstract

We calculate the 00^{++} -wave two-meson spectra for the reactions $\gamma\gamma \rightarrow \pi^0\pi^0$, $\gamma\gamma \rightarrow \pi^+\pi^-$, $\gamma\gamma \rightarrow K^0\bar{K}^0$ and $\gamma\gamma \rightarrow K^+K^-$ on the basis of: (i) the results of the K -matrix analysis of the 00^{++} amplitudes for the reactions $\pi\pi \rightarrow \pi\pi$, $K\bar{K}$, $\eta\eta$, $\eta\eta'$, $\pi\pi\pi\pi$, and (ii) recently developed method for calculation of the decay amplitudes $f_0(1^3P_0q\bar{q}) \rightarrow \gamma\gamma$, $f_0(2^3P_0q\bar{q}) \rightarrow \gamma\gamma$. The reconstructed $\pi\pi$ and $K\bar{K}$ spectra can be used as a guide for the extraction of partial widths of scalar/isoscalar resonances $f_0(980) \rightarrow \gamma\gamma$, $f_0(1300) \rightarrow \gamma\gamma$, $f_0(1500) \rightarrow \gamma\gamma$, $f_0(1750) \rightarrow \gamma\gamma$. As follows from our calculations, the resonances $f_0(980)$ and $f_0(1500)$ in the $\pi^+\pi^-$ and $\pi^0\pi^0$ spectra reveal themselves as dips.

1 Introduction

The reactions $\gamma\gamma \rightarrow mesons$ provide valuable information on the quark/gluon structure of mesonic states, see [1] and references therein. These reactions were intensively studied during the last decade (see, for example, Refs. [2-5]), and their investigations are carried on.

In the present paper we discuss the 00^{++} -spectra in the two-meson production processes $\gamma\gamma \rightarrow \pi^0\pi^0$, $\gamma\gamma \rightarrow \pi^+\pi^-$, $\gamma\gamma \rightarrow K^0\bar{K}^0$ and $\gamma\gamma \rightarrow K^+K^-$ where the production of the scalar/isoscalar resonances provides a possibility to measure partial widths $f_0 \rightarrow \gamma\gamma$.

Recently, the $\gamma\gamma$ -widths were calculated for scalar mesons, members of the $1^3P_0q\bar{q}$ and $2^3P_0q\bar{q}$ nonets [6]. In the 10^+ -channels, where scalar/isovector resonances, a_0 , are seen, the background is comparatively small. However, for scalar/isoscalar resonances there is a strong interference of the resonance signal with a background, that is quite analogous to the situation observed in the analysis of the $\pi\pi \rightarrow \pi\pi$ 00^{++} -wave at $M_{\pi\pi} \sim 600$ -1900 MeV [7,8].

Because of that, when discussing the scalar/isoscalar sector and $\gamma\gamma$ partial widths of the f_0 -states, we should reconstruct both resonance and background contributions.

There are two types of processes which determine the prompt production of mesons in the reactions $\gamma\gamma \rightarrow \pi\pi$ and $\gamma\gamma \rightarrow K\bar{K}$ (see Fig. 1 where the diagrams for the reaction $\gamma\gamma \rightarrow \pi^+\pi^-$ are shown):

- (i) direct s -channel resonance production, Fig. 1a, and
- (ii) non-resonance production (the main contribution, one can guess, is due to diagrams with the t - and u -channel pole singularities located near the physical region, Fig. 1b).

In addition, a large background in the 00^{++} -channel ultimately brings out a significant final state interaction effect.

The K -matrix approach provides an appropriate technique for taking into account both the prompt production processes and those followed by the final state meson interaction. In Refs. [7,8], the K -matrix amplitude was restored for the processes $\pi\pi \rightarrow \pi\pi$, $K\bar{K}$, $\eta\eta$, $\eta\eta'$ and $\pi\pi\pi\pi$ in the mass region $M_{\pi\pi} \leq 1900$ MeV: just this amplitude is necessary for final state interactions in the processes $\gamma\gamma \rightarrow two\ mesons$.

In the next Section we write down the K -matrix amplitudes for the processes $\gamma\gamma \rightarrow \pi\pi$ and $\gamma\gamma \rightarrow K\bar{K}$. In Section 3 the K -matrix elements for the prompt processes shown in Figs. 1a and 1b are presented. We discuss the results in Section 4, and a brief conclusion is given in Section 5.

2 K -matrix amplitudes for $\gamma\gamma \rightarrow \pi\pi$ and $\gamma\gamma \rightarrow K\bar{K}$

Here the formulae are given for the process $\gamma\gamma \rightarrow \pi^+\pi^-$; the amplitudes for other processes under consideration are written in a similar way.

The amplitude for the production of S -wave pions, with $I = 0$, in the reaction $\gamma\gamma \rightarrow \pi^+\pi^-$ reads:

$$A_{\alpha,\beta}(\gamma\gamma \rightarrow \pi^+\pi^-) = e^2 g_{\alpha\beta}^{\perp\perp} \widetilde{K}_{\gamma\gamma,a} \left(\frac{\mathbf{I}}{\mathbf{I} - i\hat{\rho}\hat{K}} \right)_{a,\pi^+\pi^-}. \quad (1)$$

The indices (α, β) refer to the photon polarization, and the metric tensor $g_{\alpha\beta}^{\perp\perp}$ works in the space perpendicular to the momenta of colliding photons. $\widetilde{K}_{\gamma\gamma,a}$ is the K -matrix element for the prompt transition $\gamma\gamma \rightarrow a$, and the index a runs over seven states: $\pi^0\pi^0$, $\pi^+\pi^-$, $K^0\bar{K}^0$, K^+K^- , $\eta\eta$, $\eta\eta'$ and $\pi\pi\pi\pi$. The factor $(\mathbf{I} - i\hat{\rho}\hat{K})^{-1}$ is responsible for the final state interaction of mesons: \mathbf{I} is

the unity matrix, $\hat{\rho}$ is the diagonal phase space matrix, $\hat{\rho} = \text{diag}(\rho_1, \rho_2, \rho_3, \dots)$, where ρ_a is the phase space of the state a , and the matrix elements K_{ab} refer to meson-meson interaction in the channels $\pi^0\pi^0$, $\pi^+\pi^-$, $K^0\bar{K}^0$, K^+K^- , $\eta\eta$, $\eta\eta'$ and $\pi\pi\pi\pi$.

2.1 K -matrix representation of the 00^{++} wave meson-meson amplitude

In the c.m. energy region $\sqrt{s} \leq 1900$ MeV, the K -matrix amplitude for meson-meson interaction in the channels $\pi\pi$, $K\bar{K}$, $\eta\eta$, $\eta\eta'$ and $\pi\pi\pi\pi$ has been found in [7] on the basis of a sample of data from Refs. [9–11]. The matrix elements were parametrized as a sum of the pole and background terms:

$$K_{ab}(s) = \sum_{\alpha} \frac{g_a^{(\alpha)} g_b^{(\alpha)}}{M_{\alpha}^2 - s} + \Phi_{ab}(s). \quad (2)$$

The analysis of Ref. [7] evidently shows that five K -matrix poles are needed for fitting to data at $\sqrt{s} \leq 1900$ MeV. The K -matrix pole corresponds to a meson state with the switched off decay channels: $g_a^{(\alpha)} \rightarrow 0$. However, the experimentally observed couplings $g_a^{(\alpha)}$ are not small, and these couplings, being responsible for the decay of meson states, are also responsible for a strong meson mixing. Moreover, the masses of mixed states differ significantly from the primary ones. These "primary mesons" were called "bare mesons" [7], in contrast to physical states, for which the cloud of real particles ($\pi\pi$, $K\bar{K}$, $\eta\eta$, and so on) plays an important role in their formation. The coupling constants of bare state, g_a^{α} , depend on quark/gluon content of the state a , so the restoration of couplings for the channels $\pi\pi$, $K\bar{K}$, $\eta\eta$, $\eta\eta'$ makes it possible to perform the $q\bar{q}$ /gluonium classification of bare 00^{++} states. The flavour content of the scalar/isoscalar bare states, members of the nonets $1^3P_0q\bar{q}$ and $2^3P_0q\bar{q}$, is determined by the mixing angle ϕ as follows: $q\bar{q} = n\bar{n} \cos \phi + s\bar{s} \sin \phi$ where $n\bar{n} = (u\bar{u} + d\bar{d})/\sqrt{2}$.

Concerning the non-pole term, a smooth s -dependence was allowed for $\Phi_{ab}(s)$.

Two solutions for the bare states in the mass region $\sqrt{s} \leq 1900$ MeV were found in Ref. [7].

Solution I:

<i>Classification</i>	<i>State</i>	<i>Mixing angle</i>	
$1^3P_0q\bar{q}$	$f_0^{\text{bare}}(720 \pm 100)$	$-69^\circ \pm 12^\circ$	
$1^3P_0q\bar{q}$	$f_0^{\text{bare}}(1260 \pm 30)$	$21^\circ \pm 12^\circ$	(3)
$2^3P_0q\bar{q}$	$f_0^{\text{bare}}(1600 \pm 50)$	$-6^\circ \pm 15^\circ$	
$2^3P_0q\bar{q}$	$f_0^{\text{bare}}(1810 \pm 30)$	$84^\circ \pm 15^\circ$	
<i>Gluonium</i>	$f_0^{\text{bare}}(1235 \pm 50)$		

Solution II:

<i>Classification</i>	<i>State</i>	<i>Mixing angle</i>	
$1^3P_0q\bar{q}$	$f_0^{\text{bare}}(720 \pm 100)$	$-69^\circ \pm 12^\circ$	
$1^3P_0q\bar{q}$	$f_0^{\text{bare}}(1260 \pm 30)$	$21^\circ \pm 12^\circ$	(4)
$2^3P_0q\bar{q}$	$f_0^{\text{bare}}(1235 \pm 50)$	$40^\circ \pm 10^\circ$	
$2^3P_0q\bar{q}$	$f_0^{\text{bare}}(1810 \pm 30)$	$-50^\circ \pm 10^\circ$	
<i>Gluonium</i>	$f_0^{\text{bare}}(1560 \pm 30)$		

Both K -matrix solutions, I and II, lead to nearly identical positions of the amplitude poles in the complex mass plane. The amplitude has five poles:

Resonance Pole position (in MeV)

$$\begin{aligned}
 f_0(980) & 1015 \pm 15 - i(43 \pm 8) \\
 f_0(1300) & 1300 \pm 20 - i(120 \pm 20) \\
 f_0(1500) & 1499 \pm 8 - i(65 \pm 10) \\
 f_0(1750) & 1750 \pm 30 - i(125 \pm 70) \\
 f_0(1530_{-250}^{+90}) & 1530_{-250}^{+90} - i(560 \pm 140) .
 \end{aligned}
 \tag{5}$$

An appearance of the broad resonance $f_0(1530_{-250}^{+90})$ is not accidental: a large width of $f_0(1530_{-250}^{+90})$ is due to an effect of the accumulation of widths of neighbouring resonances [12]. In both solutions, the broad state is the descendant of the scalar gluonium keeping $\sim 50\%$ of its component.

2.2 K -matrix elements for the transitions $\gamma\gamma \rightarrow \pi\pi$ and $\gamma\gamma \rightarrow K\bar{K}$

The K -matrix element for a prompt production of mesons, $\widetilde{K}_{\gamma\gamma,a}$ of Eq. (1), is written in a form similar to Eq. (2):

$$\widetilde{K}_{\gamma\gamma,a}(s) = \sum_{\alpha=1}^4 \frac{F_{\gamma\gamma \rightarrow f_0(\alpha)}^{\text{bare}} g_a^{(\alpha)}}{M_\alpha^2 - s} + f_{\gamma\gamma,a}. \quad (6)$$

Here $F_{\gamma\gamma \rightarrow f_0(\alpha)}^{\text{bare}}$ is the form factor for the production of bare scalar/isoscalar $q\bar{q}$ state: $\gamma\gamma \rightarrow f_0^{\text{bare}}(\alpha)$. The summation is carried over all the $q\bar{q}$ states (Eq. (3) for Solution I and Eq. (4) for Solution II). The term $f_{\gamma\gamma,a}$ refers to the background contribution.

2.3 Coupling $F_{f_0 \rightarrow \gamma\gamma}^{\text{bare}}$

In calculation of $F_{f_0 \rightarrow \gamma\gamma}^{\text{bare}}$, we follow the method developed in [6,13] where the form factors for the transition processes $meson \rightarrow \gamma^*(Q^2)\gamma$ were studied; in the limit $Q^2 \rightarrow 0$, the transition form factor provides the decay coupling $meson \rightarrow \gamma\gamma$ which is written in (6). The method is based on the double spectral representation for the transition amplitudes and application of the light-cone wave functions for mesons involved. An important point is that in the analysis of the reactions $\pi^0 \rightarrow \gamma^*(Q^2)\gamma$, $\eta \rightarrow \gamma^*(Q^2)\gamma$ and $\eta' \rightarrow \gamma^*(Q^2)\gamma$ the vertex for the transition $\gamma \rightarrow q\bar{q}$ (or photon wave function) was determined in Ref. [13].

Following the prescription of Ref. [6], we present the coupling $F_{f_0 \rightarrow \gamma\gamma}^{\text{bare}}$ in terms of the light cone variables:

$$\begin{aligned} F_{f_0 \rightarrow \gamma\gamma}^{\text{bare}} &= \frac{2\sqrt{N_c}}{16\pi^3} \int_0^1 \frac{dx}{x(1-x)^2} \int d^2k_\perp \\ &\times \left[\cos\phi Z_{n\bar{n}} T_{n\bar{n}}(x, \vec{k}_\perp) \Psi_{f_0}^{\text{bare}}(M_{n\bar{n}}^2) \Psi_{\gamma \rightarrow n\bar{n}}(M_{n\bar{n}}^2) \right. \\ &\left. + \sin\phi Z_{s\bar{s}} T_{s\bar{s}}(x, \vec{k}_\perp) \Psi_{f_0}^{\text{bare}}(M_{s\bar{s}}^2) \Psi_{\gamma \rightarrow s\bar{s}}(M_{s\bar{s}}^2) \right]. \quad (7) \end{aligned}$$

Here x and k_\perp^2 are the light cone variables of quarks; $\Psi_{f_0}^{\text{bare}}(M_{q\bar{q}}^2)$ is the $q\bar{q}$ wave function of f_0^{bare} , and $M_{q\bar{q}}^2$ is the $q\bar{q}$ invariant mass squared for strange, $M_{s\bar{s}}^2$, or non-strange, $M_{n\bar{n}}^2$, quarks:

$$M_{q\bar{q}}^2 = \frac{m^2 + k_\perp^2}{x(1-x)}. \quad (8)$$

Here m is the constituent quark mass; $Z_{n\bar{n}}$ and $Z_{s\bar{s}}$ are charge factors for $n\bar{n}$ and $s\bar{s}$ components: $Z_{n\bar{n}} = (e_u^2 + e_d^2)/\sqrt{2} = 5/9\sqrt{2}$ and $Z_{s\bar{s}} = e_s^2 = 1/9$. The factor $\sqrt{N_c}$, where $N_c = 3$ is the number of colours, is related to the normalization of the photon vertex; the photon wave functions $\Psi_{\gamma \rightarrow n\bar{n}}(M_{n\bar{n}}^2)$ and $\Psi_{\gamma \rightarrow s\bar{s}}(M_{s\bar{s}}^2)$ were found in Ref. [13].

The wave function f_0^{bare} of the basic nonet $1^3P_0q\bar{q}$ is parametrized in the exponential form:

$$\Psi_{f_0}^{\text{bare}}(M_{q\bar{q}}^2) = C e^{-bM_{q\bar{q}}^2}, \quad (9)$$

where C is normalization constant, and the parameter b determines the radius squared of the bare state.

The wave function of the first radial excitation, $2^3P_0q\bar{q}$, is written in the exponential approximation as follows:

$$\Psi_{f_0}^{\text{bare}(1)}(M_{q\bar{q}}^2) = C_1(D_1M_{q\bar{q}}^2 - 1)e^{-b_1M_{q\bar{q}}^2}. \quad (10)$$

The parameter b_1 can be related to the radius of the radial excitation state, then the values C_1 and D_1 are fixed by the normalization and orthogonality requirements, $\Psi_{f_0}^{\text{bare}(1)} \otimes \Psi_{f_0}^{\text{bare}(1)} = 1$ and $\Psi_{f_0} \otimes \Psi_{f_0}^{\text{bare}(1)} = 0$.

For the transition form factor, the spin structure factor $T_{n\bar{n}}(x, \vec{k}_\perp)$ is fixed by the quark loop trace. It is equal to [6]:

$$T_{q\bar{q}}(x, \vec{k}_\perp) = 2mM_{q\bar{q}}^2 \left[1 + \frac{k_\perp^2 \cos^2 \varphi}{M_{q\bar{q}}^2(1-x)^2} \right]^{-1} - 8m^3, \quad (11)$$

where $\vec{k}_\perp = (k_\perp \sin \varphi, k_\perp \cos \varphi)$.

2.4 Background terms $f_{\gamma\gamma,a}$

The background terms cannot be calculated unambiguously, they are to be considered as free parameters. One may suggest that dominant contribution into $f_{\gamma\gamma,a}$ is given by pole diagrams with t - and u -channel singularities located near the physical region: these are diagrams of Fig. 1b type with charged pion and kaon exchanges. However, the pole terms contain unknown t - and u -channel form factors: in the pole diagram of Fig. 1b, the form factor refers to the $\gamma\pi\pi$ -vertex. These form factors cause uncertainties in calculation of the pole diagram contributions into $f_{\gamma\gamma,a}$.

Below, when estimating $\pi\pi$ and $K\bar{K}$ spectra, we follow an idea that dominant contribution comes from the processes with charge exchanges in the crossing t - and u -channels. Therefore $f_{\gamma\gamma,\pi^+\pi^-} \neq 0$ and $f_{\gamma\gamma,K^+K^-} \neq 0$, while all other $f_{\gamma\gamma,a}$'s are equal to zero. We parametrize $f_{\gamma\gamma,\pi^+\pi^-}$ in the form:

$$f_{\gamma\gamma,\pi^+\pi^-} = \zeta_{\pi\pi} \frac{\pi}{\sqrt{3}} \int_{-1}^1 dy \left[1 + \frac{s(s-4\mu^2)(1-y^2)}{s^2 - s(s-4\mu^2)y^2} \right]. \quad (12)$$

Here $\zeta_{\pi\pi}$ is a parameter, the factor $1/\sqrt{3}$ is Clebsch-Gordon coefficient, and μ is the pion mass. The integral in (12) is the S -wave projection of the sum of the pion exchange diagrams in t - and u -channels: we fix the s -dependent shape of $f_{\gamma\gamma,\pi^+\pi^-}$ in a form which is given by the closest pole terms in the t - and u -channels. The parameter $\zeta_{\pi\pi}$ effectively accounts for the uncertainties related to the contributions of form factors and other more distant diagrams.

The background term $f_{\gamma\gamma,K^+K^-}$ is parametrized by the analogous expression, with the replacements $\zeta_{\pi\pi}/\sqrt{3} \rightarrow \zeta_{K\bar{K}}/\sqrt{2}$ and $\mu \rightarrow \mu_K$.

3 Results

The results of calculation of the 00^{++} -wave two-meson spectra in the reactions $\gamma\gamma \rightarrow \pi^0\pi^0$, $\gamma\gamma \rightarrow \pi^+\pi^-$, $\gamma\gamma \rightarrow K^0\bar{K}^0$ and $\gamma\gamma \rightarrow K^+K^-$ are shown in Figs. 2 to 5.

For the calculation of spectra, we fix the parameters b and b_1 which determine the radii of mesons $1^3P_0q\bar{q}$ and $2^3P_0q\bar{q}$, see Eqs. (9) and (10). The value b is chosen to be the same as that of $a_0(980)$: following the results of Refs. [7,8], we suppose that $a_0(980)$ is a member of the $1^3P_0q\bar{q}$ nonet. The calculation of partial width $a_0(980) \rightarrow \gamma\gamma$ gives [6]: $R^2(1^3P_0q\bar{q}) \sim 15 \text{ GeV}^{-2}$. The quark model teaches us that the meson radius for the first radial excitation should be greater than that of the basic nonet; correspondingly, we put $R^2(2^3P_0q\bar{q}) = 22 \text{ GeV}^{-2}$. In terms of a pion radius, it means that $R(1^3P_0q\bar{q})/R_\pi \simeq 1.22$ and $R(2^3P_0q\bar{q})/R_\pi \simeq 1.48$. The couplings $F_{f_0(\alpha) \rightarrow \gamma\gamma}^{\text{bare}}$ are calculated for these values of radii.

The parameters $\zeta_{\pi\pi}$ and $\zeta_{K\bar{K}}$ define the background in the $\pi\pi$ and $K\bar{K}$ spectra. We use the data from the low-energy region of spectra $\gamma\gamma \rightarrow \pi\pi$ (where the S -wave dominates) to fix $\zeta_{\pi\pi}$. However, in this region the data of different groups differ significantly from each other, so we present in Figs. 2 to 5 the calculation results with $\zeta_{\pi\pi} = 0.5$ and $\zeta_{\pi\pi} = 0.35$ which provide better description of either the data of Ref. [2] or Ref. [4], correspondingly.

A relative sign of the wave functions $\Psi_{f_0}^{\text{bare}}$ and $\Psi_{f_0}^{\text{bare}(1)}$ is not fixed. Two curves in Figs. 2 to 5, solid and dotted ones, correspond to opposite signs of C_1 .

In all calculation variants the resonances $f_0(980)$ and $f_0(1500)$ reveal themselves as dips in the $\pi^0\pi^0$ and $\pi^+\pi^-$ spectra; the resonance $f_0(1300)$ is hardly seen producing rather weak variations in the spectra. At $E > 1000$ MeV, the contribution of the 02^{++} -wave increases being dominant in the region of the $f_2(1270)$ -resonance.

For the $K\bar{K}$ spectra, we consider the variants with $\zeta_{\pi\pi} = 0.5$, $\zeta_{K\bar{K}} = 0.7$ (Figs. 4a,b and 5a,b) and $\zeta_{\pi\pi} = 0.35$, $\zeta_{K\bar{K}} = 0.44$ (Figs. 4c,d and 5c,d). The variant $\zeta_{\pi\pi} = 0.5$, $\zeta_{K\bar{K}} = 0.7$ supposes that the contribution of the 02^{++} -wave into K^+K^- spectrum is small at 1200-1400 MeV. More realistic is the variant with $\zeta_{\pi\pi} = 0.35$, $\zeta_{K\bar{K}} = 0.44$ where the peak in the region 1300 MeV is due to the $f_2(1270)$ -resonance. The 00^{++} -wave gives a small contribution to the $K^0\bar{K}^0$ spectrum, see Fig. 5, (the resonance $a_0(980)$ can dominate in the region near 1000 MeV).

4 Conclusion

The extraction of partial widths $f_0(980) \rightarrow \gamma\gamma$ and $f_0(1500) \rightarrow \gamma\gamma$ from studying the reactions $\gamma\gamma \rightarrow \pi\pi$ and $\gamma\gamma \rightarrow K\bar{K}$ requires detailed partial wave analysis of meson spectra. Here the situation is similar to that in the spectra $\pi\pi \rightarrow \pi\pi$: the resonances $f_0(980)$ and $f_0(1500)$ reveal themselves as dips in both reactions.

The $\pi\pi$ and $K\bar{K}$ spectra are not sensitive to the position of a pure gluonium: solutions I and II, which refer to pure gluonium at 1230 and 1600 MeV, correspondingly, give rather similar spectra. The unification of the spectra with different positions of the gluonium is due to the final state interaction effects.

We thank D.V. Bugg, L.G. Dakhno, V.A. Nikonov and A.V. Sarantsev for useful discussions and comments. The paper was supported by grants RFFI 98-02-17236 and INTAS-RFBR 95-0267.

References

- [1] T. Barnes, *Theoretical Aspects of Light Meson Spectroscopy*, in: Hadron Spectroscopy and the Confinement Problem, Edited by D.V. Bugg, Plenum Press, New York (1996);

- E. Klempt, *Hadron '97 Summary*, in: Hadron Spectroscopy, AIP Conference Proceedings 432, Editors S.-U. Chung and H.J. Willutzki, Woodbury, New York (1998).
- [2] T. Oest et al. (JADE Coll.) Z. Phys. **C47** (1990) 343.
- [3] D. Morgan, M. Pennington, Z. Phys. **C48** (1990) 623.
- [4] D. Antreasyan et al. (Crystal Ball Coll.) Phys. Rev. **D33** (1986) 1847;
H. Mariske et al. (Crystal Ball Coll.) Phys. Rev. **D41** (1990) 3324.
- [5] C. Caso et al. (PD Group), Eur. Phys. J. **C3**, (1998) 1.
- [6] A.V. Anisovich, V.V. Anisovich, D.V. Bugg, V.A. Nikonov, *Partial widths $a_0(980) \rightarrow \gamma\gamma$, $f_0(980) \rightarrow \gamma\gamma$ and $q\bar{q}$ classification of the lightest scalar mesons*, hep-ph 9903396, Phys. Lett. **B**, in press.
- [7] V.V. Anisovich, Yu.D. Prokoshkin, A.V. Sarantsev, Phys. Lett. **B389** (1996) 388.
- [8] V.V. Anisovich, A.A. Kondashov, Yu.D. Prokoshkin et al. *Two-pion spectra for the reaction $\pi^- p \rightarrow \pi^0 \pi^0 n$ at 38 GeV/c pion momentum and combined analysis of the GAMS, Crystal Barrel and BNL data*, hep-ph/9711319, unpublished.
- [9] D. Alde et al. (GAMS), Zeit. Phys. **C66** (1995) 375;
Yu. D. Prokoshkin et al. (GAMS), Physics-Doklady **342** (1995) 473;
F. Binon et al. (GAMS), Nuovo Cim. **A78**, 313 (1983); **A80** (1984) 363.
- [10] S. J. Lindenbaum and R. S. Longacre, Phys. Lett. **B274** (1992) 492;
A. Etkin et al., Phys. Rev. D **25** (1982) 1786.
- [11] V.V. Anisovich et al. (Crystal Barrel Coll.), Phys. Lett. **B323** (1994) 233;
C. Amsler et al. (Crystal Barrel Coll.), Phys. Lett. **B342** (1995) 433; **B355** (1995) 425.
- [12] V.V. Anisovich, D.V. Bugg, A.V. Sarantsev, Phys. Rev. **D 58**:111503 (1998).
- [13] V.V. Anisovich, D.I. Melikhov, V.A. Nikonov, Phys. Rev. **D55** (1997) 2918 ;
Phys. Rev. **D52** (1995) 5295;
V.V. Anisovich, D.V. Bugg, D.I. Melikhov, V.A. Nikonov, Phys. Lett. **B404** (1997) 166.

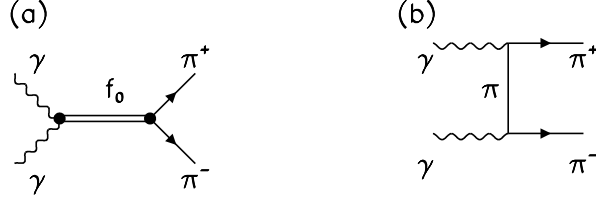


Fig. 1. Diagrams for the prompt production of $\pi^+\pi^-$: a) s -channel f_0 -meson production, b) t -channel (or u -channel) π -meson exchange process.

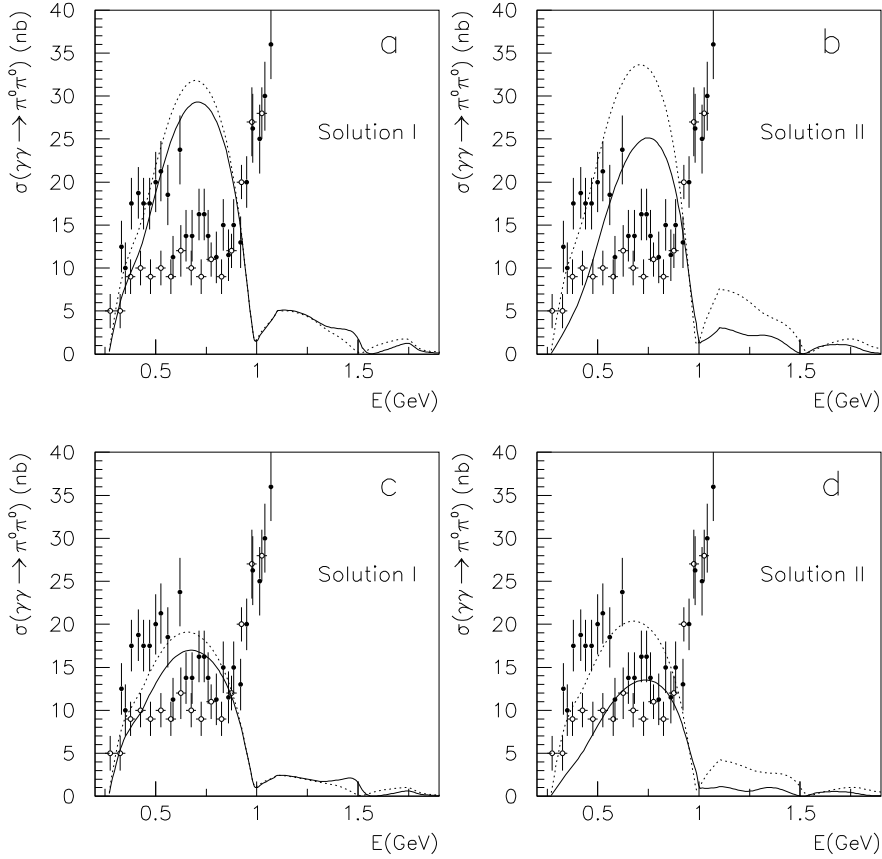


Fig. 2. The 00^{++} cross section for $\gamma\gamma \rightarrow \pi^0\pi^0$ reaction. Solid and dashed curves correspond to positive and negative signs of the normalization constant for the first radial excitation wave function; $\zeta_{\pi\pi} = 0.5$ stands for (a) and (b), and $\zeta_{\pi\pi} = 0.35$ for (c) and (d). Experimental data are taken from Refs. [2,4]: the data include contributions of all waves.

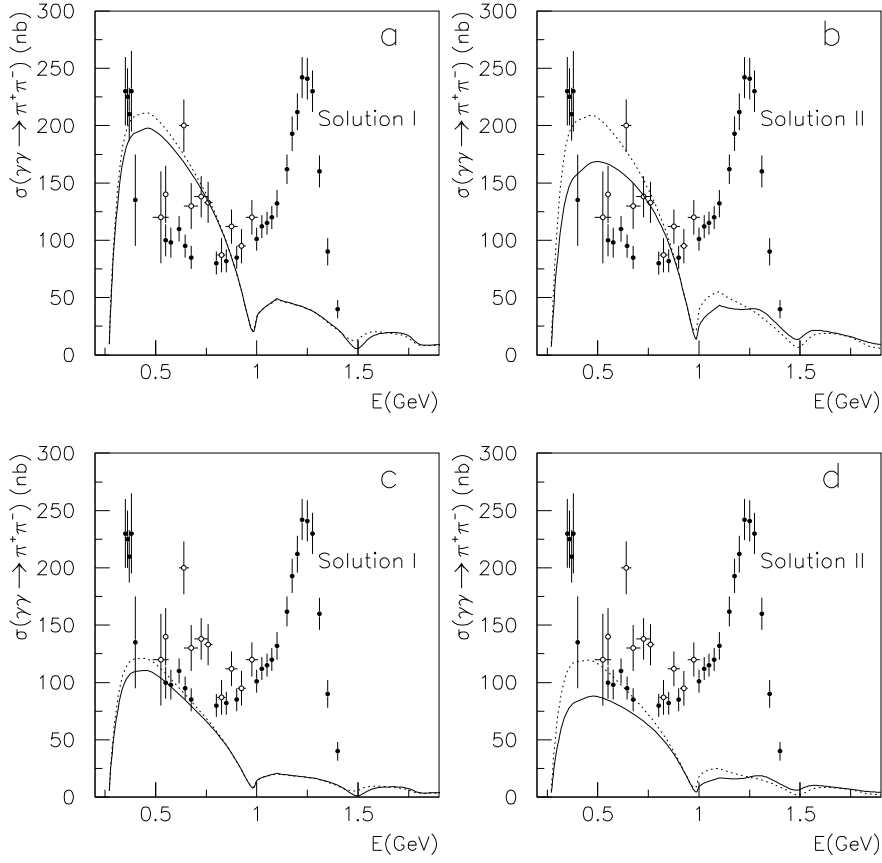


Fig. 3. The 00^{++} cross section for $\gamma\gamma \rightarrow \pi^+\pi^-$ reaction. Notations are the same as for Fig. 2.

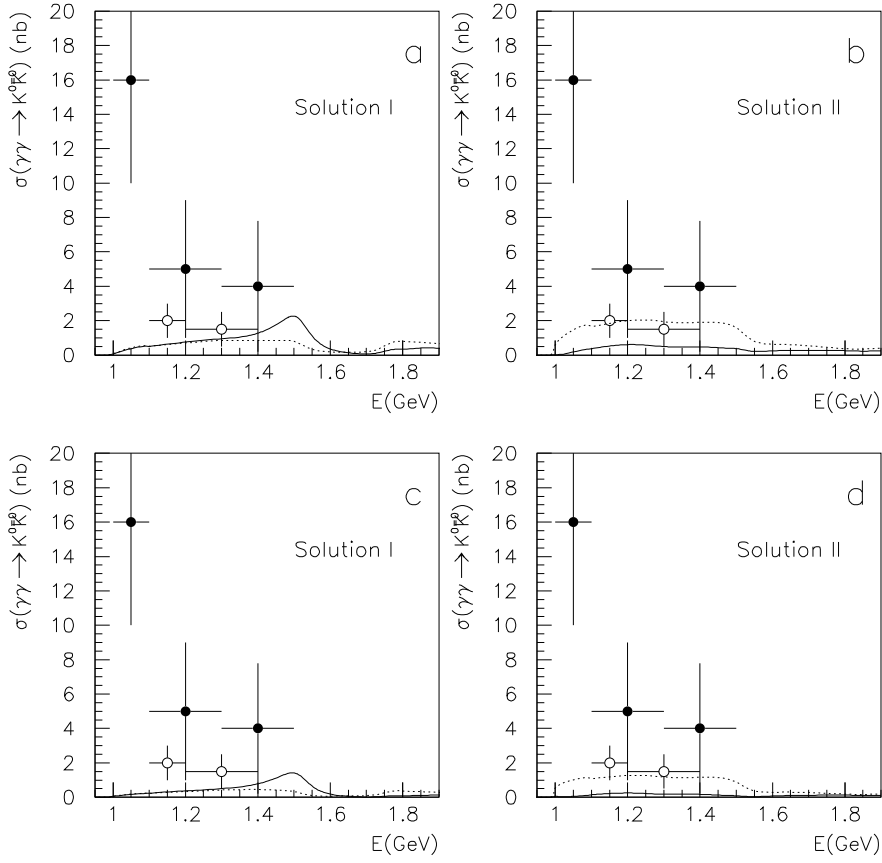


Fig. 4. The 00^{++} cross section for $\gamma\gamma \rightarrow K^0\bar{K}^0$ reaction. Curves are marked as in Fig. 2; (a) and (b) correspond to $\zeta_{\pi\pi} = 0.5$, $\zeta_{K\bar{K}} = 0.7$ and (c) and (d) correspond to $\zeta_{\pi\pi} = 0.35$, $\zeta_{K\bar{K}} = 0.44$.

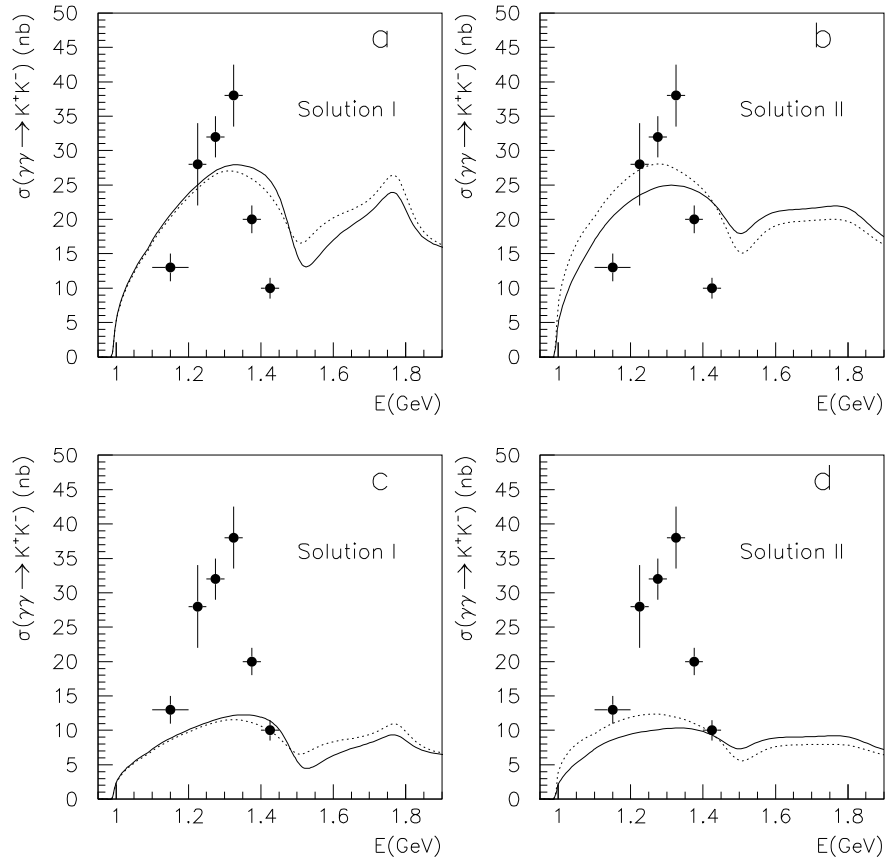


Fig. 5. The 00^{++} cross section for $\gamma\gamma \rightarrow K^+K^-$ reaction. Notations are the same as in Fig. 4.